A COMPARATIVE ANALYSIS OF LOW-THRUST AND NEPTUNE GRAVITY-ASSIST STRATEGIES FOR REDIRECTING TRANS-NEPTUNIAN OBJECTS TO MARS*

A. Hess

Faculty of Physics, University of Warsaw
Pasteura 5, 02-093 Warsaw, Poland

R. Gabryszewski, L. Czechowski

Space Research Centre of the Polish Academy of Sciences
Bartycka 18A, 00-716 Warsaw, Poland

Received 22 February 2026, accepted 9 April 2026, published online 2 July 2026

We investigate the feasibility of redirecting trans-Neptunian objects (TNOs) from the Kuiper Belt to Mars using sustained low-thrust propulsion combined with a single Neptune gravity assist. Numerical trajectory optimisation with global derivative-free solvers shows that carefully phased low-thrust control can reduce the required ΔV to approximately 2.5–3.2 $\mathrm{km\,s^{-1}}$ for transfer times of several centuries. For the higher-eccentricity test case, a well-timed Neptune flyby further lowers the propulsive cost, whereas for the lower-eccentricity case, it yields only marginal savings at the expense of a longer transfer time. We illustrate the sensitivity to the initial semi-major axis, eccentricity, and inclination, describe the trade-off between pre- and post-assist control effort, and discuss structural and operational limitations. The results suggest dynamical accessibility for inward volatile delivery from the outer Solar System within an idealized model.

DOI:10.5506/APhysPolBSupp.19.3-A2

1. Introduction

Obtaining enough water is one of the most important challenges in the context of long-term plans to terraform Mars. Water, alongside carbon dioxide, is a fundamental factor necessary to initiate geochemical and climatic processes leading to the permanent maintenance of atmosphere and a stable hydrological cycle on the planet's surface [1]. Contemporary terraforming

* Presented at the Planetary Science Conference, Kraków, Poland, 23–25 October, 2025.

concepts assume several potential sources of water acquisition — from melting existing ice resources in the Martian cryosphere, through chemical production, to delivering volatile substances from external regions of the Solar System [2].

The quantitative scale of the problem is formidable: increasing the present Martian atmospheric mass ($\sim 2.5 \times 10^{16}$ kg) to even the modest pressures required for the Armstrong limit or for pure-oxygen breathing would necessitate importing 10^{17}–10^{18} kg of volatiles [3]. These numbers are mainly meant to motivate, but they also make one thing clear: you need a sufficiently large reservoir of volatiles. The Kuiper Belt, with a total mass of order a few hundredths of an Earth mass, is one of the largest reservoirs of icy material in the outer Solar System. Its low-density objects preserve substantial amounts of H_2O, CO_2, CO, NH_3, and other ices; cometary measurements, including those for 67P/Churyumov–Gerasimenko, provide an important example of volatile-rich small body composition [4, 5]. Thus, from a mass-budget perspective, trans-Neptunian bodies are attractive candidates for a large-scale volatile delivery.

A typical trans-Neptunian object needs to move from about 30–100 AU down to 1.5 AU, which requires a very large change in orbital energy. Impulsive propulsion may work for a spacecraft, but it is unlikely to be practical for kilometre-scale natural bodies due to their high inertia and limited structural integrity [6]. Continuous low thrust — possibly realizable in the future with high-specific-impulse energy sources [7] — can generate only minute accelerations, but over centuries it can slowly change the trajectory and create a favourable geometry for a planetary encounter. A single gravity assist from a giant planet, particularly Neptune, can reduce the heliocentric energy more efficiently than thrust alone, provided that the encounter geometry is favourable [8].

The concept of employing large-scale engineering to render Mars more habitable has a long history. One of the first important estimates came from Zubrin and McKay [1], who combined a model of the Martian CO_2 system with a simplified astrodynamical analysis. It has been estimated that redirecting an icy body from beyond Jupiter (using its own volatiles as propellant) would require a ΔV of $\sim 300\ \mathrm{m\,s^{-1}}$. That value is approximate, but it helped open the discussion on outer-Solar-System sources for terraforming. Later work refined these ideas. Czechowski [9] emphasized the enormous energetic costs of raising the pressure on Mars to even one-tenth that of Earth, showing that Kuiper Belt objects are the most likely source of unstable elements, but become dynamically brittle as they are transported inward. Pałka, Olszewski, and Wendland [10] applied spatial data science and numerical modelling based on the Mars Global Climate Model/Mars Climate Database to simulate atmospheric changes in Mars-terraformation scenarios

with rapid impact-driven greenhouse-gas release and slow greenhouse-gas production, and to compare their energy requirements. On the other hand, geomorphological and remote sensing research has further emphasized the relationship between subsurface and atmospheric processes [11, 12]. Theoretical models of controlled extraterrestrial habitats [13] further demonstrate the relationship between terraforming claims and models of planetary engineering.

Against this backdrop, we analyzed this transport problem from a strictly dynamical perspective. Most earlier approaches relied on simplified impulse transfers — Hohmann or bi-elliptic [14] — but those only hold for circular, coplanar orbits. Our work instead combines heliocentric two-body propagation under low-thrust control with a patched-conic approximation for a Neptune gravity assist. This study intends to fill that gap by determining the control effort needed to place a trans-Neptunian object on a Mars-directed trajectory illustrating how this requirement depends on the initial semi-major axis, eccentricity, and inclination, and evaluating whether a single Neptune flyby provides a practically advantage over optimized direct low-thrust control in terms of both ΔV and transfer duration. Using only the dynamical component, we find the range of distances from which volatile-rich bodies can be brought from beyond the orbit of Neptune.

2. Methods

For this proof-of-concept study, two representative test bodies were chosen to reflect typical orbits from the Kuiper Belt and the scattered disk. Do not consider this sample to be a statistical survey of the trans-Neptunian population — it is only meant to illustrate the dependence of transfer performance on initial eccentricity and inclination. Their initial osculating elements at the epoch are listed in Table 1.

Table 1. Initial osculating orbital elements of the two representative test bodies. Longitude of ascending node Ω, argument of perihelion ω, and true anomaly ν are set to 0° for both objects.

Parameter	Unit	TB #1 (KBO)	TB #2 (SDO)
Semi-major axis a	AU	45.00	80.00
Eccentricity e	—	0.20	0.50
Inclination i	deg	10.00	35.00

The first body (TB #1) is a classical Kuiper Belt Object with medium eccentricity and inclination. The second body (TB #2) is a Scattered Disk

Object with a larger semi-major axis, higher eccentricity, and higher inclination, which influences transfer energetics and the geometry of potential gravity-assist encounters.

Various thrust strategies were tested, ranging from continuous, purely retrograde thrusting oriented opposite the instantaneous velocity vector to fully optimized, piecewise-constant control vectors. A nominal acceleration scale of 4×10^{-10} km s^{-2} was adopted in all low-thrust simulations, chosen to represent an extremely weak but sustained propulsion level that lies far beyond current practical capabilities for kilometre-scale natural bodies, although not for spacecraft low-thrust propulsion as such [9]. In each transfer leg, we optimized the Cartesian components of the control-acceleration vector within bounded intervals. As a result, the effective acceleration magnitude depended on the solution and should be understood as being on the order of the adopted nominal scale, rather than as a strictly fixed value throughout the transfer. In the numerical model,

$$\boldsymbol{a}_{\mathrm{T}} = f_{\mathrm{T}}\,\boldsymbol{u}\,, \qquad \boldsymbol{u} = (u_x, u_y, u_z)\,, \qquad u_x, u_y, u_z \in [-1, 1]\,,$$

with $f_{\mathrm{T}} = 4 \times 10^{-10}$ km s^{-2}. For a given transfer leg of duration Δt, the reported control effort was evaluated as

$$\Delta V = \int_0^{\Delta t} \|\boldsymbol{a}_{\mathrm{T}}\|\,\mathrm{d}t = f_{\mathrm{T}}\,\|\boldsymbol{u}\|\,\Delta t\,,$$

since $\boldsymbol{u}$ was held constant within that leg.

The two test trajectories were chosen to illustrate how initial eccentricity and inclination trade against required ΔV and transfer time. In general, higher initial eccentricity and a smaller perihelion distance may both favour inward transfer, because they reduce the geometric change required to bring the body toward the inner Solar System. A broader assessment of the general usefulness of Neptune assistance would require a larger ensemble of initial conditions and is left for future work.

To optimize the control vector and the parameters of the Neptune flyby, we used advanced mathematical algorithms that do not require calculating derivatives of the target function. These methods are well-suited for complex problems with a multi-peaked structure, where many local solutions exist and the search space is discontinuous.

One of the methods employed was the CMA-ES algorithm (Covariance Matrix Adaptation Evolution Strategy), which adapts its operation to the local shape of the search area, ensuring reliable convergence even for high-dimensional problems [15]. The second method was the DE algorithm (Differential Evolution), a population-based approach that is particularly effective at exploring widely separated regions of the search space [16].

For each fixed transfer time, the objective function minimized the terminal miss distance to the prescribed target state (either a Neptune encounter proxy or the position of Mars). Among the resulting solutions, only those satisfying the adopted terminal collision criterion in the heliocentric model,

$$\|\boldsymbol{r}_{\mathrm{obj}}(t_0 + \Delta T) - \boldsymbol{r}_{\mathrm{Mars}}(t_0 + \Delta T)\| \leq R_{\mathrm{Mars}}\,,$$

were classified as Mars-impacting. The corresponding ΔV was then evaluated from the optimized control vector. The reported ΔV values therefore correspond to best-found collisional trajectories for the sampled transfer durations, rather than to formal global minima of ΔV.

For gravity-assist modelling, we first identified epochs and initial conditions that permit an exact Neptune intercept in the heliocentric model. These Neptune-intercept solutions were then used as encounter seeds for constructing nearby flyby geometries. For each candidate encounter geometry, we sampled flyby parameters (close-approach scale and orientation in the b-plane) and computed the post-encounter asymptotic states using a patched-conic approximation. The post-assist trajectories were then continued under low-thrust using a propagator that integrates the heliocentric equations of motion until Mars impact or until failure criteria were met.

3. Results

3.1. Retrograde-thrust deceleration

The simplest control strategy we examined is continuous retrograde thrust, in which the acceleration vector always points opposite to the instantaneous orbital velocity. This lowers the specific orbital energy of the body and causes its trajectory to spiral gradually inwards towards the Sun.

With each successive revolution, the osculating semi-major axis shrinks in a stepwise fashion, with each step marking the passage of one orbital period. The process is more pronounced if the initial eccentricity is large, as this means that the thrust acts over a larger range of heliocentric distances. The time evolution of the osculating eccentricity in the retrograde-thrust case has an oscillatory initial phase. This is due to the interaction between the semi-major axis and the eccentricity under a non-central perturbation. Depending on the instantaneous geometry, the anti-tangential force either increases or decreases the osculating eccentricity. Once the body approaches the inner Solar System, the evolution becomes monotonic, with eccentricity steadily increasing. The reason is that retrograde thrust applied near perihelion reduces the orbital angular momentum more efficiently than it removes energy, leading to secular growth in eccentricity. The corresponding evolution of the osculating orbital elements is shown in Fig. 1.

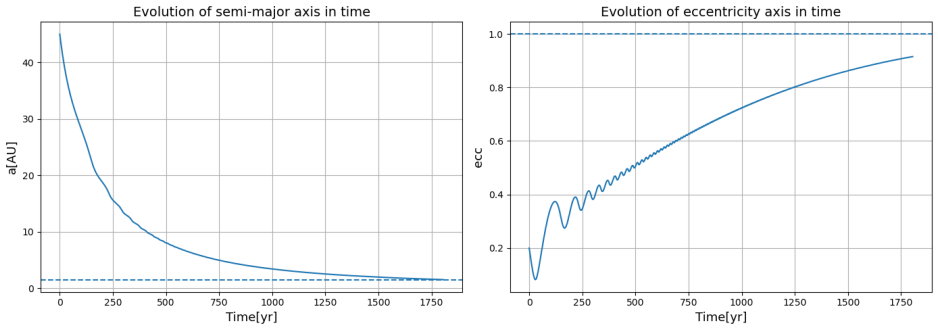

Fig. 1. Osculating orbital elements evolution as a function of time for the simple retrograde-thrust deceleration applied to TB #1. The plot shows the slow decline of the semi-major axis and the evolution of eccentricity during the prolonged deceleration phase.

The trajectory projected onto the orbital plane traces out an inward spiral. Each loop corresponds to a complete revolution, with the radius shrinking as the orbital energy is dissipated. Because the thrust remains confined to the instantaneous orbital plane, the inclination is unchanged, and the spiral is planar. The loops progressively tighten as the trajectory approaches the heliocentric distance of Mars, 1.52 AU. The corresponding heliocentric XY-plane trajectory is shown in Fig. 2.

For TB #1, this straightforward strategy proved highly inefficient energetically, requiring $\Delta V = 22.8$ km/s and a transfer time of 1800 years to approach the heliocentric distance of Mars. Such excessive cost results not from exceptionally large heliocentric speeds in the outer Solar System, but from the inefficiency of purely retrograde steering for reshaping the trajectory and lowering the perihelion under extremely weak acceleration. Moreover, the secular changes are small per unit time, which explains the very long mission duration. In addition, continuous retrograde thrust does not take advantage of favorable planetary geometry and thus misses the large momentum exchange that could be obtained from gravity assist. In conclusion, retrograde-only deceleration is not a viable option in realistic mission planning when other assist or optimized direction strategies exist.

3.2. Optimized low-thrust transfer

The CMA-ES and DE methods were used to optimize the weak control vector for fixed transfer durations greatly reducing the ΔV. The optimization allowed for the control acceleration to be pointed in non-intuitive directions (not strictly retrograde) using phasing effects which reduce the overall impulse needed to lower perihelion and target Mars. The best-found colli-

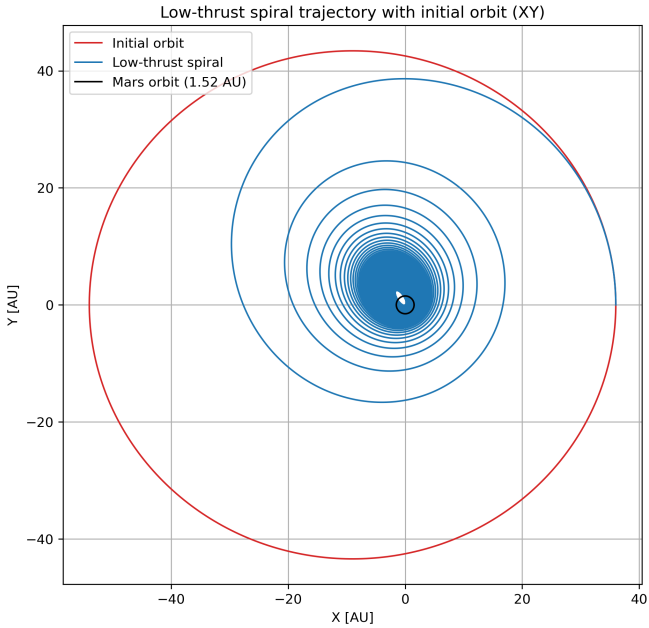

Fig. 2. Trajectory of TB #1 in the heliocentric XY plane under simple retrograde thrust. The figure shows a slow inward drift and a geometry that is not well-suited for planetary encounters.

sional trajectories for the sampled transfer durations produced the following representative results:

— TB #1: $\Delta V = 3.18$ km/s for $\Delta T = 384$ years.
— TB #2: $\Delta V = 2.50$ km/s for $\Delta T = 480$ years.

The values show that a precise timing and control of the low-thrust trajectory direction are essential to approach energy-efficient transfer solutions.

3.3. Neptune gravity-assist results

The hybrid strategy combines a continuous low thrust and a single close encounter with Neptune, to take advantage of the gravity field of the planet to decrease the heliocentric energy without using propellant during the flyby, when the geometry is advantageous. The perihelion of the orbit is pulled closer into the inner Solar System as the body passes the planet and its incoming velocity vector is turned.

The low-thrust acceleration has two main objectives: to place the body on the right trajectory for the Neptune encounter, and, after the flyby, to correct the trajectory to end with an impact on Mars. The gravity assist does most of the work in reorienting the trajectory, while the thrust mainly supplies the corrections needed for accurate targeting.

We turned to a patched-conic approximation in the poliastro library to model the flyby manoeuvre [17]. In the planet-centred frame, the incoming and outgoing asymptotic speeds are equal, v_{rel}, and the encounter rotates the relative velocity by a scattering angle δ. The outgoing relative velocity is just a rotated version of the incoming vector,

$$\boldsymbol{v}_{\mathrm{rel}}^{+} = \boldsymbol{R}\left(\hat{\boldsymbol{k}}, \delta\right)\, \boldsymbol{v}_{\mathrm{rel}}^{-}\,,$$

and the post-encounter heliocentric velocity is the sum of Neptune's heliocentric velocity and the outgoing relative velocity,

$$\boldsymbol{v}_{\mathrm{hel}}^{+} = \boldsymbol{v}_{N} + \boldsymbol{v}_{\mathrm{rel}}^{+}\,,$$

where $\boldsymbol{v}_{\mathrm{N}}$ is Neptune's heliocentric velocity. The encounter changes the heliocentric specific energy by

$$\Delta\varepsilon = \frac{1}{2}\left(\left|\boldsymbol{v}_{\mathrm{hel}}^{+}\right|^{2} - \left|\boldsymbol{v}_{\mathrm{hel}}^{-}\right|^{2}\right) = \boldsymbol{v}_{\mathrm{N}}\,\left(\boldsymbol{v}_{\mathrm{rel}}^{+} - \boldsymbol{v}_{\mathrm{rel}}^{-}\right)\,,$$

and the corresponding change in the osculating semimajor axis follows from $\varepsilon = -\mu_{\odot}/(2a)$ (for small $\Delta\varepsilon$, we can use $\Delta a \approx \frac{2a^{2}}{\mu_{\odot}}\,\Delta\varepsilon$). In the optimisation, the scattering geometry get defined using the b-plane azimuth ϕ and a characteristic close-approach distance. This lets us rotate $\boldsymbol{v}_{\mathrm{rel}}^{-}$ and obtain the post-flyby state for subsequent low-thrust propagation.

For the classical Kuiper Belt Object (TB #1), the optimization yielded a trajectory in which the body reaches Neptune after 250 years of low-thrust guidance, requiring a cumulative control effort of $\Delta V_1 = 2.79$ km/s. Following the encounter, a relatively short post-assist leg of 171 years, needing only $\Delta V_2 = 0.32$ km/s, brings the object to Mars. Compared to the pure optimization of the low-thrust solution for TB #1 ($\Delta V = 3.18$ km/s over 384 years), the Neptune-assisted transfer offers only a marginal propulsive gain at the expense of 37 years of mission duration. In this lower-eccentricity case, the operational justification for the added complexity of the gravity-assist strategy does not appear to be there.

The scattered-disk object (TB #2) needed a longer pre-flyby phase of 430 years to build up $\Delta V_1 = 1.96$ km/s for a favourable encounter geometry with a characteristic flyby distance of $20\,R_N$ and orientation $\phi = 20°$. After the assist, a terminal leg of 110 years with $\Delta V_2 = 0.23$ km/s completed the

transfer. The total $\Delta V = 2.19$ km/s over 540 years is less than the purely optimized low-thrust transfer for this body (2.50 km/s) with only a modest 12.5% increase in mission duration. This demonstrates that for the more eccentric of the two tested cases, a well-timed gravity assist can outperform carefully optimized continuous thrust alone.

The latter was found to be inversely proportional to the former, *i.e.* the control effort before the flyby (ΔV_1) and after the flyby (ΔV_2). This indicates that for the more eccentric of the two tested cases, an early gravity assist can be better than a well optimized constant thrust only. Trajectories that reach Neptune with a small ΔV_1 often leave the encounter on a path that still needs significant correction to reach Mars, which drives ΔV_2 up. On the other hand, using more propulsive work before the gravity assist can place the body on a better post-encounter trajectory and reduce the final correction cost. Finding the right balance between these two is a key part of the optimization.

In general, a higher initial eccentricity and a smaller perihelion distance favour inward transfers, because they reduce the geometric change needed to move the body toward the inner Solar System. In the two cases discussed here, the lower ΔV for TB #2 is not due to a smaller initial perihelion distance — in fact, its initial q is larger than that of TB #1. Instead, the

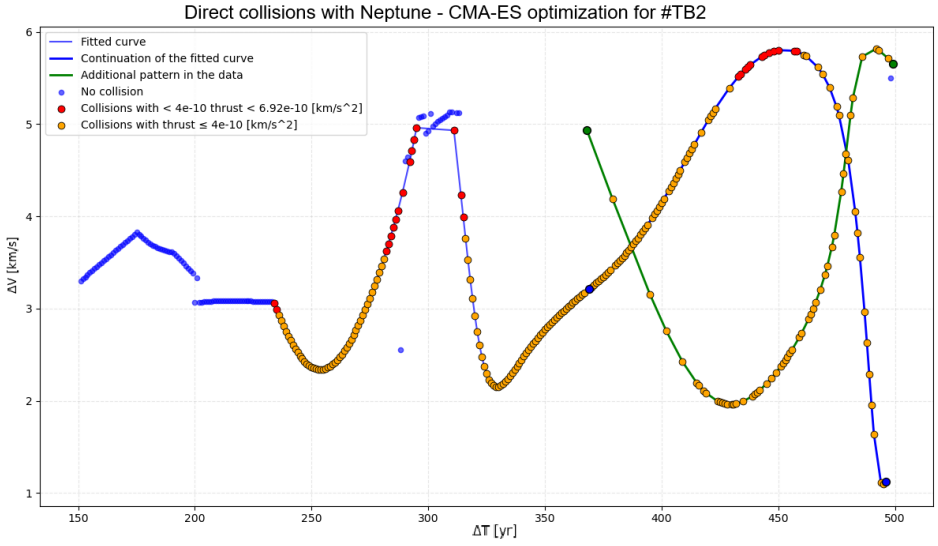

Fig. 3. How total ΔV changes over time for Neptune-intercept "seeds" that were then screened for nearby flyby geometries and Mars targeting. The pattern of distinct curves is a result of the set of encounter "seed" solutions. The fitted curve shows what the geometry tends to drive.

improvement comes from combining a more elongated initial osculating orbit with the encounter geometry chosen in the optimization. For TB #2, this combination works particularly well with the Neptune flyby and yields the lowest overall ΔV among all strategies considered. The dependence of the total ΔV on the transfer time for the Neptune-intercept seed solutions is shown in Fig. 3. The corresponding optimized TB #2 flyby trajectory is shown in Fig. 4, while the evolution of the osculating orbital elements over the full manoeuvre is shown in Fig. 5.

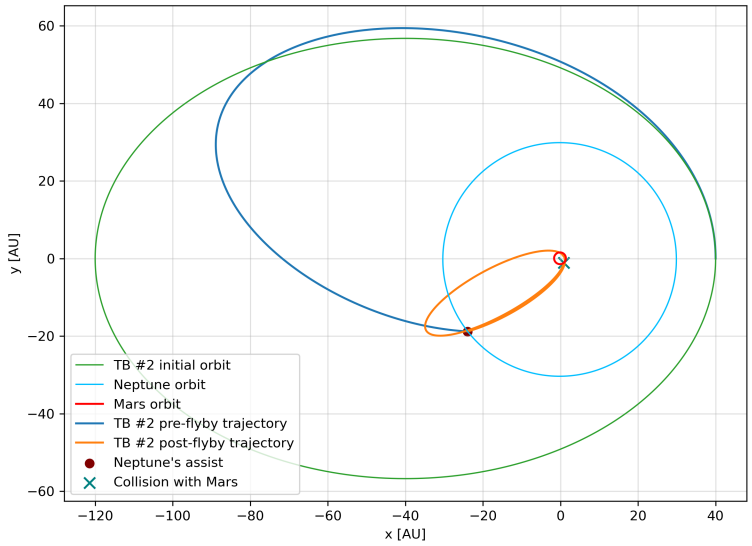

Fig. 4. Here is the initial osculating orbit of TB #2 (SDO), the low-thrust inbound trajectory to Neptune for gravity assist, and the post-assist path all the way to impact on Mars. The sharp deflection at the encounter with Neptune and the subsequent inward motion of the body towards Mars are clearly visible.

4. Conclusions

We have demonstrated that it is dynamically possible to redirect trans-Neptunian objects toward Mars by using optimized low-thrust propulsion combined with a single gravity assist near Neptune. This result applies within our simplified model, namely a heliocentric two-body framework with a patched-conic flyby approximation. Within this framework, the redirection problem is dynamically accessible. This was shown by solving the equations of motion under continuous weak control and by using global optimization algorithms in the adopted heliocentric model.

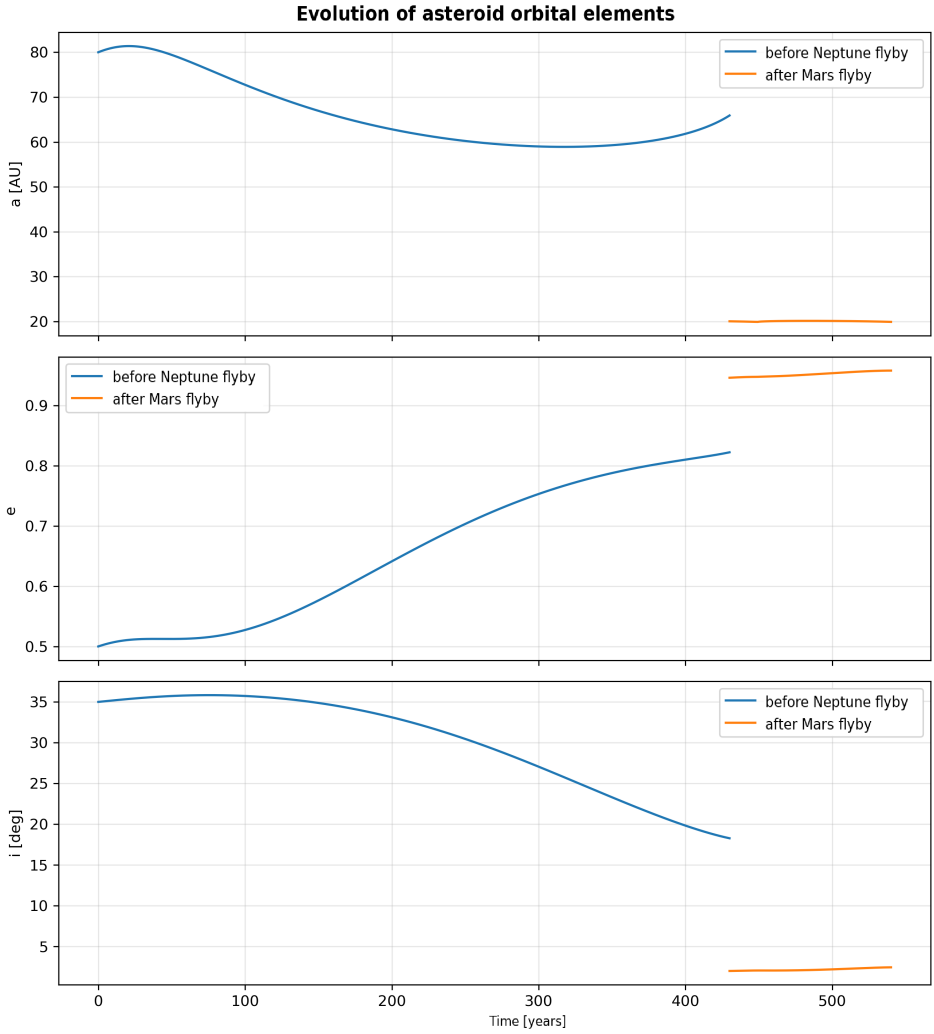

Fig. 5. Time evolution of the osculating orbital parameters (semi-major axis, eccentricity, inclination) over the entire manoeuvre for TB #2, including the gravity-assist event and the subsequent low-thrust phase. The sharp changes at the time of the flyby and the more gradual variation during thrusting are visible.

We have allowed the control direction to vary instead of fixing it in a retrograde direction, which dramatically reduces the required velocity increment. For the representative optimized transfers, the required ΔV drops to 3.18 $\mathrm{km\,s^{-1}}$ for TB #1 and 2.50 $\mathrm{km\,s^{-1}}$ for TB #2. In comparison, the retrograde TB #1 case requires 22.8 $\mathrm{km\,s^{-1}}$ and $\sim$ 1800 years to reach

the heliocentric distance of Mars. This leads to better control efficiency and shows the importance of the phasing of the thrust direction and of the orbital dynamics, rather than only energy dissipation.

A Neptune gravity assist can provide additional benefits, but its usefulness depends on the case. For the lower-eccentricity TB #1 case, the gravity assist provides little benefit: the total ΔV decreases only slightly, from 3.18 $\mathrm{km\,s^{-1}}$ to 3.11 $\mathrm{km\,s^{-1}}$, while the transfer time increases from 384 to 421 years. For the scattered-disk TB #2 case, the hybrid approach gives a clearer improvement, reducing ΔV from 2.50 $\mathrm{km\,s^{-1}}$ to 2.19 $\mathrm{km\,s^{-1}}$ with only a small increase in transfer time. The added complexity of using a gravity assist is justified only for favourable initial trajectories. When this happens, the flyby reduces heliocentric energy without using propellant during the encounter. As for low thrust, its main role is to guide the object to the correct encounter conditions and then clean up the trajectory afterward. If less control effort is applied before the flyby, more is usually needed after it. This compromise has to be carefully weighed during trajectory design.

The initial orbital parameters, particularly eccentricity, exert a strong influence on the transfer economics. In general, higher initial eccentricity and smaller perihelion distance can facilitate inward transport under optimized low-thrust control. In the two representative cases analysed here, the more eccentric SDO-like starting configuration yielded a lower total ΔV than the KBO-like case, even though the two test cases also differ in semi-major axis and inclination. These results suggest that some scattered-disk-like starting geometries may be attractive targets for inward volatile transport. Every optimized trajectory takes several centuries to complete. This raises questions about the technological and programmatic viability of maintaining low-thrust missions over such long periods. While the adopted nominal acceleration scale of 4×10^{-10} $\mathrm{km\,s^{-2}}$ lies far beyond current practical capabilities for kilometer-scale natural bodies, it can still serve as a plausible benchmark for future high-specific-impulse systems that might rely on in-situ resource utilisation or large-scale ablation techniques. Taken together, these results provide an idealized dynamical baseline for the controlled return of volatile-rich bodies from the region beyond Neptune.

Further study should consider the following limitations of the current model. The neglect of planetary perturbations implies that the calculated ΔV values should be interpreted as optimistic lower-bound estimates, and a complete N-body solution involving time-dependent control adjustments would probably require more control action. The effects of errors in the guidance and navigation solutions and the ephemerides of both the target and Neptune must be assessed. Finally, exploring sequences of multiple gravity assists or combined flybys of several giant planets could yield even more efficient transfer solutions. Since only two representative initial con-

ditions were analyzed, the present results should be interpreted as a proof of concept rather than as a population-wide assessment of trans-Neptunian transfer opportunities. Despite these caveats, the present study suggests that, from a purely dynamical perspective and within an idealized model, trans-Neptunian objects may constitute a long-term source of water and volatiles for future Mars terraforming concepts.

REFERENCES

[1] R. Zubrin, C. McKay, «Technological requirements for terraforming Mars», in: «Proceedings of the 29th Joint Propulsion Conference and Exhibit», No. AIAA-93-2005, Monterey, CA, USA, 28–30 June, 1993. Published by the American Institute of Aeronautics and Astronautics, Inc.

[2] P.T. Metzger, *Space Policy* **37**, 77 (2016).

[3] H. Hargitai, A. Kereszturi, «Encyclopedia of Planetary Landforms», *Springer*, New York, NY 2015.

[4] G. Filacchione *et al.*, *Space Sci. Rev.* **215**, 19 (2019).

[5] M. Rubin *et al.*, *Space Sci. Rev.* **216**, 102 (2020).

[6] E.Y. Choueiri, *Sci. Am.* **300**, 58 (2009).

[7] T.W. Glover, «VASIMR VX-200 Performance and Near-term SEP Capability for Mars Cargo Flights», presented at the Future In-Space Operations Seminar, 19 January, 2011, DOI: 10.13140/RG.2.2.12214.83528.

[8] L. Czechowski, *Earth Moon Planets* **52**, 113 (1991).

[9] L. Czechowski, «Energy problems of terraforming Mars», presented at the 56th Lunar and Planetary Science Conference, The Woodlands, TX, USA, 10–14 March, 2025; see also A. Tomaswick, *Universe Today*, 7 April, 2025.

[10] P. Pałka, R. Olszewski, A. Wendland, *Energies* **15**, 4957 (2022).

[11] L. Czechowski *et al.*, «The formation of cone chains in the Chryse Planitia region on Mars and the thermodynamic aspects of this process», *Icarus* **396**, 115473 (2023).

[12] L. Czechowski, «Terraforming Mars — a feasibility study», presented at the Planetary Science Conference, Kraków, Poland, 23–25 October, 2025, not included in the proceedings.

[13] A. Adler, *Centaurus* **62**, 763 (2020).

[14] R.F. Hoelker, R. Silber, «The bi-elliptical transfer between circular coplanar orbits», Technical Report TN D-235, NASA, 1961.

[15] N. Hansen, `arXiv:1604.00772 [cs.LG]`.

[16] R. Storn, K. Price, *J. Global Optim.* **11**, 341 (1997).

[17] J.L. Cano Rodríguez *et al.*, «poliastro/poliastro: poliastro 0.17.0 (SciPy US'22 edition)», Zenodo, 2023, DOI: 10.5281/zenodo.6817189.